TWO-PHOTON "GHOST" IMAGE AND INTERFERENCE-DIFFRACTION

Y.H. Shih, A.V. Sergienko, T.B. Pittman, D.V. Strekalov, and D.N. Klyshko[1]

Department of Physics, University of Maryland Baltimore County
Baltimore, MD 21228, U.S.A.

1 Introduction

One of the most surprising consequences of quantum mechanics is the entanglement of two or more distant particles. The two-particle entangled state was mathematically formulated by Schrödinger [1]: Consider a pure state for a system composed of two spatially separated subsystems,

$$\rho = |\Psi\rangle\langle\Psi| \; ; \quad |\Psi\rangle = \sum_{a,b} c(a,b)|a\rangle|b\rangle \tag{1}$$

where $|a\rangle$ and $|b\rangle$ are two sets of orthogonal vectors for subsystem 1 and 2. If $c(a,b)$ does not factor into a product of the form $f(a) \times g(b)$, so that the state does not factor into a product state for subsystem 1 and 2 (e.g. $\rho \neq \rho_1 \otimes \rho_2$), the state is defined by Schrödinger as an "entangled state".

The classic example of a two-particle entangled state was suggested by Einstein, Podolsky, and Rosen in their famous 1935 *gedankenexperiment* [2]:

$$|\Psi\rangle = \sum_{a,b} \delta(a + b - c_o)|a\rangle|b\rangle \tag{2}$$

where c_o is a constant. What is surprising about the entangled state (2) is the following: *the measured value of an observable for either single subsystem is undeterminate. However, if one of the subsystems is measured to be at a certain value for that observable (the measured value is certainly an eigen value) the other one is 100% determinate.* This point can be easily seen from the delta function in state (2). Based on this unusual quantum behavior, EPR defined their "physical reality" and then asked the question: "Can Quantum-Mechanical Description of Physical Reality Be Considered Complete [3]?" One may not appreciate EPR's criterian of physical reality and insist that "no elementary quantum phenomenon is a phenomenon until it is a recorded phenomenon" [4], however, no one can ignore the unusual nonlocal behavior of state (2), especially considering when the measurements of subsystems 1 and 2 are space-like separated events.

Optical spontaneous parametric down conversion (SPDC) [5] [6] is the most effective mechanism to generate an EPR type entangled two-photon state. In SPDC, an optical beam, called the pump, is incident on a birefringent crystal. The pump is intense enough so that nonlinear effects lead to the conversion of pump photons into pairs of photons, historically called signal and idler.

---

[1]Permanent address: Department of Physics, Moscow State University, Moscow, Russia

The two-photon state generated from the SPDC crystal may be calculated from the standard theory (first order perturbation theory) to be [6],

$$|\Psi\rangle = \sum_{s,i} \delta(\omega_s + \omega_i - \omega_p)\delta(\mathbf{k}_s + \mathbf{k}_i - \mathbf{k}_p)a_s^\dagger\left(\omega_s(\mathbf{k}_s)\right) a_i^\dagger\left(\omega_i(\mathbf{k}_i)\right)|0\rangle \qquad (3)$$

where ω and $\mathbf{k}$ represent the frequency and the wave vector for signal (s), idler (i), and pump (p). The two delta functions in state (3) are usually explicitly written as phase matching conditions:

$$\omega_s + \omega_i = \omega_p , \quad \mathbf{k}_s + \mathbf{k}_i = \mathbf{k}_p \qquad (4)$$

Technically, the SPDC is said to be type I or type II, depending on whether the signal and idler beams have parallel or orthogonal polarization. The SPDC conversion efficiency is typically on the order of 10^{-9} to 10^{-11}, depending on the SPDC nonlinear material. The signal and idler intensities are extremely low, only single photon detection devices can register them. It is clear that state (3) is an EPR type two-photon entangled state. The quantum entanglement nature of SPDC has been demonstrated in EPR-Bohm experiments and Bell's inequality measurements [7]. The following two experiments were recently performed in our laboratory, which are more closely related to the original 1935 EPR *gedankenexperiment*.

The first experiment is a two-photon optical imaging type experiment [8], which has been named "ghost image" by the physics community. The *signal* and *idler* beams of SPDC are sent in different directions, so that the detection of the *signal* and *idler* photons can be performed by two distant photon counting detectors. An aperture object (mask) is placed in front of the *signal* photon detector and illuminated by the *signal* beam through a convex lens. Surprisingly, an image of this aperture is observed in the *idler* beam, by scanning the *idler* photon detector in the transverse plane of the *idler* beam, if we are sure that the *idler* photon detector "catches" the "twin brother" of the *signal*, which can be easily performed by a coincidence measurement. This effect is even more striking when we found that the object-lens-image relationship satisfies the *Gaussian thin lens equation*.

The second experiment demonstrates two-photon "ghost" interference-diffraction [9]. The experimental set up is similar to the image experiment, except that rather than a lens and an aperture it is a Young's double-slit (or a single-slit) inserted into the path of the *signal* beam. We could not find any interference (or diffraction) pattern behind the slit. Surprisingly, an interference (or diffraction) pattern is observed when scanning the detector in the *idler* beam, if we are sure that the *idler* photon detector "catches" the "twin brother" of the *signal*.

2 Two-photon "ghost" image experiment

The experimental set-up is shown in fig. 1. The $351.1nm$ line of an Argon Ion laser is used to pump a nonlinear BBO (β-BaB_2O_4) crystal which is cut at a degenerate Type-II phase matching angle to produce pairs of orthogonally polarized signal (e-ray of the BBO) and idler (o-ray of the BBO) photons [5]. The pairs emerge from the crystal near collinearly, with $\omega_s \cong \omega_i \cong \omega_p/2$, where ω_j ($j = s, i, p$) is the frequency of the signal, idler, and pump, respectively. The pump is then separated from the down conversion beam by a UV grade fused silica dispersion prism and
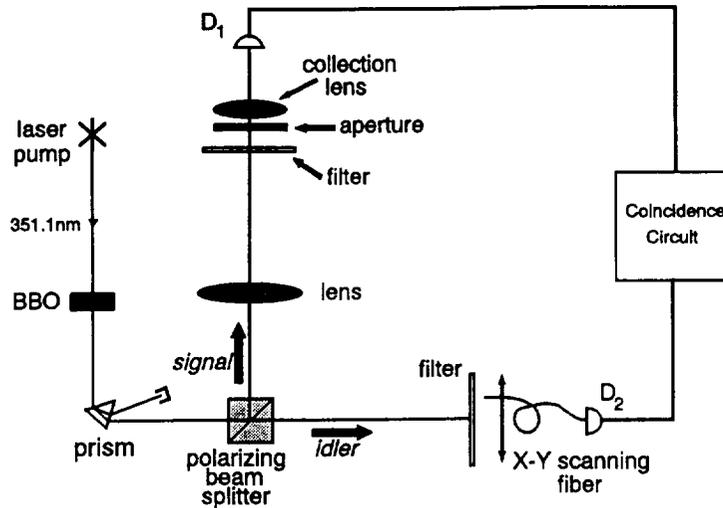
FIG.1. A schematic set-up for the two-photon "ghost" image experiment

the remaining signal and idler beams are sent in different directions by a polarization beam splitting Thompson prism. The signal beam passes through a convex lens with a $400mm$ focal length and illuminates a chosen aperture (mask). As an example, one could choose the letters "UMBC". Behind the aperture is the detector package D_1, which consists of a $25mm$ focal length collection lens in whose focal spot is a $0.8mm$ diameter dry ice cooled avalanche photodiode. The idler beam is met by detector package D_2, which consists of a $0.5mm$ diameter multi-mode fiber whose output is mated with another dry ice cooled avalanche photodiode. The input tip of the fiber is scanned in the transverse plane by two encoder drivers, and the output pulses of each detector, which are operating in the Geiger mode, are sent to a coincidence counting circuit with a $1.8ns$ acceptance window. Both detectors are preceded by $83nm$ bandwidth spectral filters centered at the degenerate wavelength, $702.2nm$.

By recording the coincidence counts as a function of the fiber tips' transverse plane coordinates, we see the image of the chosen aperture (for example "UMBC"), as is reported in fig. 2. It is
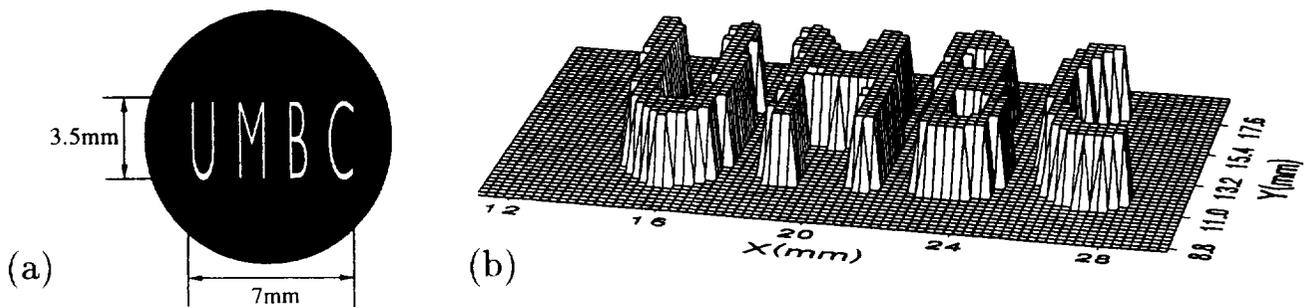

FIG.2. a) A reproduction of the actual aperture "UMBC" placed in the signal beam. Note that the size of the letters is on the order of standard text. b) The image of "UMBC": coincidence counts as a function of the fiber tip's transverse plane coordinates. The scanning step size is 0.25mm. The data shown is a "slice" at the half maximum value, with no image enhancement.

interesting to note that while the size of the "UMBC" aperture inserted in the signal beam is only about $3.5mm$ X $7mm$, the observed image measures $7mm$ X 14mm. We have therefore managed linear magnification by a factor of 2. Despite the completely different physical situation, the remarkable feature here is that *the relationship between the focal length of the lens f, the aperture's optical distance from the lens S, and the image's optical distance from the lens (lens back through beamsplitter to BBO then along the idler beam to the image) S' satisfies the Gaussian thin lens equation*:

$$\frac{1}{S} + \frac{1}{S'} = \frac{1}{f} \tag{5}$$

In this experiment, we chose $S = 600mm$, and the twice magnified clear image was found when the fiber tip was in the plane with $S' = 1200mm$ (see fig.3).

To understand this unusual phenomenon, we examine the quantum nature of the two-photon state produced in SPDC, which is entangled in momentum. The spatial distribution of the photon pairs is the result of the *transverse* components of the wave vector condition in equation (4) and Snell's law upon exiting the crystal:

$$k_s \sin \alpha_s = k_i \sin \alpha_i \longrightarrow \omega_s \sin \beta_s = \omega_i \sin \beta_i \tag{6}$$

where α_s and α_i are the scattering angles inside the crystal and β_s and β_i are the exit angles of the signal and idler photons with respect to the k_p direction. Therefore, near the degenerate case the photons constituting one pair are emitted at roughly equal, yet opposite, angles relative to the pump. Although the momentum of each photon is indeterminate, if one is measured at a certain value then the other is 100% determined. This then allows for a simple explanation of the experiment in terms of "usual" geometrical optics in the following manner: considering the action of the beamsplitter, we envision the crystal as a "hinge point" and "unfold" the schematic of fig. 1 into that shown in fig. 3. Because of the equal angle requirement of equation (6), we see that
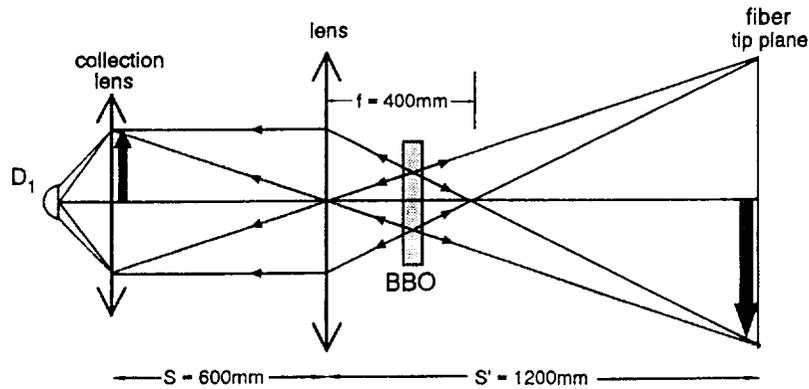

FIG.3. A conceptual "unfolded" version of the schematic shown in fig. 1, which is helpful for understanding the physics. Although the placement of the lens and the detectors obey the Gaussian thin lens equation, it is important to remember that the geometric rays actually represent pairs of SPDC photons which propagate in different directions.

all photon pairs which result in a coincidence detection can be represented by *straight lines* (but keep in mind the different propagation directions) and therefore the image is well produced in coincidences when the aperture, lens, and fiber tip are located according to equation (5). In other words, the image is exactly the same as one would observe on a screen placed at the fiber tip if detector D_1 were replaced by a point-like light source and the BBO crystal by a reflecting mirror [10].

3 "Ghost" interference-diffraction

The schematic experimental set-up is illustrated in fig. 4. It is similar to the first experiment except that after the separation of signal and idler, the signal photon passes through a double-silt (or single-slit) aperture and then travels about $1m$ to meet a point-like photon counting detector D_1 (0.5mm in diameter). The idler photon travels a distance about $1.2m$ from BS to the input tip of the optical fiber. In this experiment only the horizontal transverse coordinate, x_2, of the fiber input tip is scanned by an encoder driver.
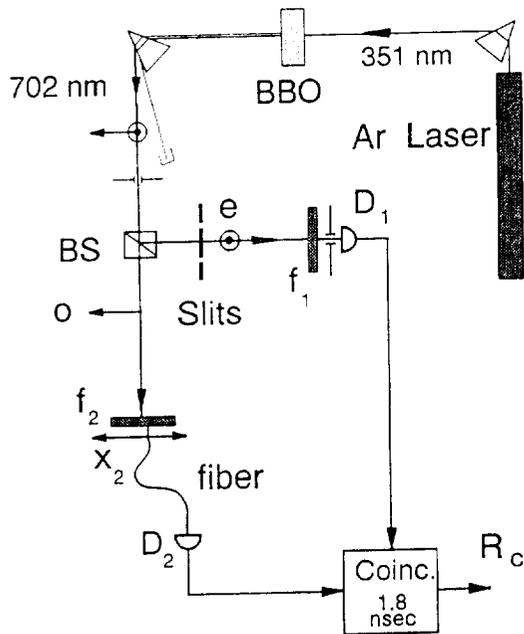
FIG.4.   A schematic set-up for the two-photon "ghost" interference-diffraction experiment. The signal (e-ray of BBO) and idler (o-ray of BBO) photon pair is generated in nonlinear crystal BBO. The ultra violet pump beam is separated from the down conversion beams by a UV grade fused silica dispersion prism. BS is a beamsplitting Thompson prism for splitting the signal and idler beams to different directions. f_1 and f_2 are spectral filters with 702.2nm center wavelength and 10nm bandwidth. Both photon counting detectors D_1 and D_2 are dry ice cooled avalanche photodiode operated in Geiger mode.

Fig. 5 reports a typically observed double-slit interference-diffraction pattern. The coincidence counting rate is reported as a function of x_2, which is obtained by scanning the detector D_2 (the fiber tip) in the idler beam, whereas the double-slit is in the signal beam. The Young's double-silt has a slit-width $a = 0.15mm$ and slit-distance $d = 0.47$mm. The interference period is measured to be $2.7 \pm 0.2mm$ and the half-width of the envelope is estimated to be about 8mm.
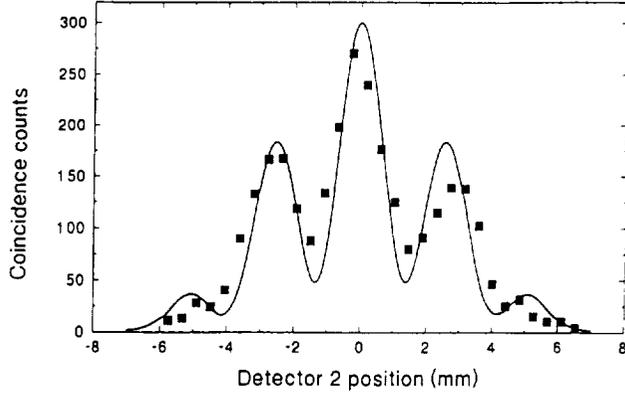
FIG.5. Typically observed interference-diffraction pattern: the dependence of the co-incidences (per 400 sec) on the position of optical fiber tip of detector D_2, which counts the idler photons, while the signal photons pass through a double-slit with $a = 0.15mm$ and $d = 0.47mm$. The solid curve is calculated from equation (7).
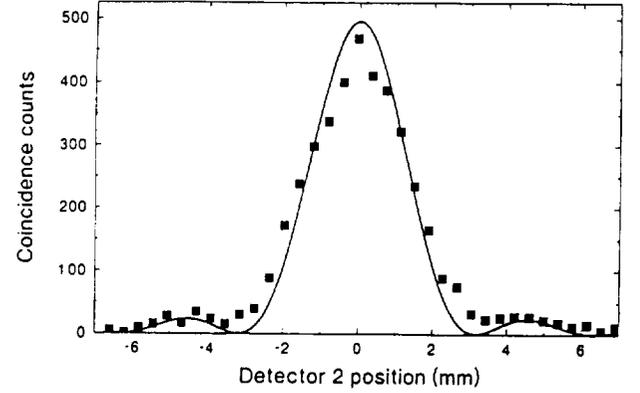
FIG.6. Two-photon diffraction: coincidence counts (per 400 sec) vs. the idler photon counting detector position. A single slit of width $a = 0.4mm$ is in the signal beam. The solid curve is a fit from the theoretical calculations.

By curve fittings, we conclude that the observation is a standard Young's interference-diffraction pattern:

$$R_c(x_2) \propto sinc^2\left(\frac{x_2\pi a}{\lambda z_2}\right) \cos^2\left(\frac{x_2\pi d}{\lambda z_2}\right). \tag{7}$$

The remarkable feature here is that z_2 *is the distance from the slits plane, which is in the signal beam, back through BS to BBO crystal and then along the idler beam to the scanning fiber tip of detector* D_2 (see fig. 4). The calculated interference period and the half-width of the sinc function from equation (7) are $2.67mm$ and $8.4mm$, respectively. Even though the interference-diffraction pattern is observed in coincidences, *the single detector counting rates are both observed to be constant when scanning detector* D_1 *or* D_2. Of course it is reasonable not to have any first order interference-diffraction in the single counting rate of D_2, which is located in the "empty" idler beam. Of interest, however, is that the absence of the first order interference-diffraction structure in the single counting rate of D_1, which is behind the double-slit, is mainly due to the divergence of the SPDC beam ($\gg \lambda/d$). In other words, the "blurring out" of the first order interference fringes is due to the considerably large momentum uncertainty of a single SPDC photon.

Furthermore, if D_1 is moved to an unsymmetrical point, which results in unequal distances to the two slits, the interference-diffraction pattern is observed to be simply shifted from the current symmetrical position to one side of x_2. This is quite mind boggling: *imagine* that there were a first order interference pattern behind the double-slit and D_1 were moved to a completely destructive interference point (i.e. zero intensity at that point) and fixed there. Can we still observe the same interference pattern in the coincidences (same period, shape, and counting rate), except for a phase shift?

174

Fig. 6 reports a typical single-slit diffraction pattern. The slit-width $a = 0.4mm$. The pattern fits to the standard diffraction sinc function, i.e., the "envelope" of equation (7), within reasonable experimental error. Here again z_2 is the unusual distance described in the above paragraphs.

To explain this unusual phenomenon, we again present a simple quantum model where, similar to the "ghost" image experiment, the momentum of either single photon is undeterminate. However, if one is measured at a certain value the other one is determinate with unit probability. This important peculiarity selects the only possible optical paths in fig. 7, when one photon passes through the double-slit aperture while the other gets to D_2. In the near degenerate case, we can simply treat the crystal as a reflecting mirror.
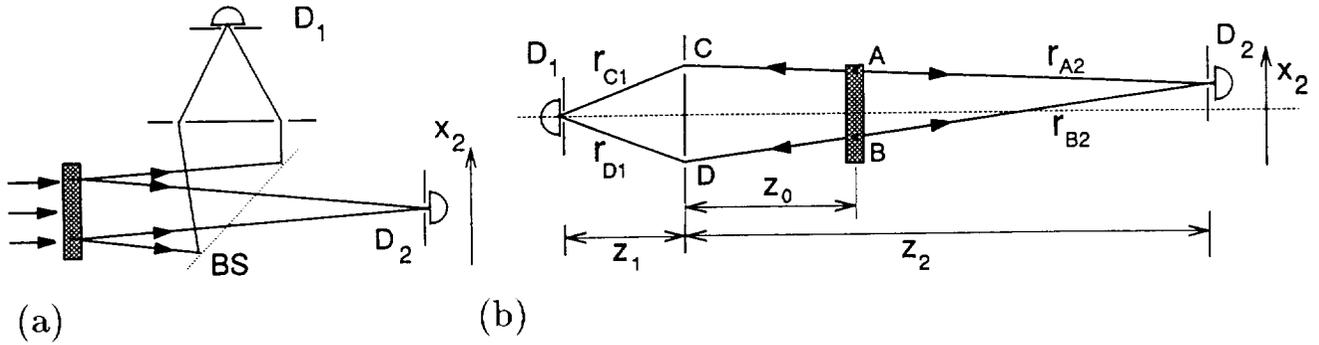

(a)   (b)

FIG.7: a) Simplified experimental scheme, and b) its "unfolded" version . The overall optical path lengths between D_1 and D_2 along the upper (r_A) and lower (r_B) paths, appearing in equation (11), are defined as: $r_A \equiv r_{A1} + r_{A2} = r_{C1} + r_{C2}$, and $r_B \equiv r_{B1} + r_{B2} = r_{D1} + r_{D2}$, where r_{Ci} and r_{Di} are the optical path lengths from the slits C and D to the ith detector.

The coincidence counting rate R_c is determined by the probability P_{12} of detecting a pair of photons by detectors D_1 and D_2 simultaneously. For SPDC, P_{12} is proportional to the square of the second order correlation function $\langle E_2^{(+)} E_1^{(+)} \rangle$ of the fields at points D_1 and D_2 (it thus plays the role of the two-photon effective wavefunction):

$$P_{12} = \langle E_1^{(-)} E_2^{(-)} E_2^{(+)} E_1^{(+)} \rangle = |\langle E_2^{(+)} E_1^{(+)} \rangle|^2. \tag{8}$$

In equation (8) $\langle \ldots \rangle \equiv \langle \Psi | \ldots | \Psi \rangle$, and $|\Psi\rangle$ is the four-mode state-vector of the SPDC field:

$$|\Psi\rangle = |vac\rangle + \epsilon \left[a_s^\dagger a_i^\dagger e^{i\phi_A} + b_s^\dagger b_i^\dagger e^{i\phi_B} \right] |vac\rangle \tag{9}$$

where $\epsilon \ll 1$ is proportional to the pump field (classical) and the nonlinearity of the crystal, ϕ_A and ϕ_B are the phases of the pump field at A and B, and a_j^+ (b_j^+) are the photon creation operators for the upper (lower) mode in fig. 7b (j = s, i). In terms of the Copenhagen interpretation one may say that the interference is due to the uncertainty in the birth-place (A or B in fig. 7) of a photon pair.

In equation (8) the fields at the detectors are given by

$$E_1^{(+)} = a_s e^{ikr_{A1}} + b_s e^{ikr_{B1}} \quad ; \quad E_2^{(+)} = a_i e^{ikr_{A2}} + b_i e^{ikr_{B2}} \tag{10}$$

where r_{Ai} (r_{Bi}) are the optical path lengths from region A (B) along the upper (lower) path to the ith detector. Substituting equations (9) and (10) into equation (8),

$$R_c \propto P_{12} = \epsilon^2 |e^{i(kr_A+\phi_A)} + e^{i(kr_B+\phi_B)}|^2 \propto 1 + \cos[k(r_A - r_B)] \qquad (11)$$

where we assume $\phi_A = \phi_B$ in the second line of equation (11) (although this is not a necessary condition to see the interference pattern, the transverse coherence of the pump beam at A and B is crucial). In equation (11) we defined the overall optical lengths between the detectors D_1 and D_2 along the upper and lower paths (see fig. 7b): $r_A \equiv r_{A1}+r_{A2} = r_{C1}+r_{C2}$, $r_B \equiv r_{B1}+r_{B2} = r_{D1}+r_{D2}$, where r_{Ci} and r_{Di} are the path lengths from the slits C and D to the ith detector.

If the optical paths from the fixed detector D_1 to the two slits are equal, i.e., $r_{C1} = r_{D1}$, and if $z_2 \gg d^2/\lambda$, then $r_A - r_B = r_{C2} - r_{D2} \cong x_2 d/z_2$ and equation (11) can be written as

$$R_c(x_2) \propto \cos^2\left(\frac{x_2 \pi d}{\lambda z_2}\right). \qquad (12)$$

Equation (12) has the form of standard Young's double-slit interference pattern. Here again z_2 is the unusual distance from the slits plane, which is in the signal beam, back through BS to the crystal and then along the idler beam to the scanning fiber tip of detector D_2.

If the optical paths from the fixed detector D_1 to the two slits are unequal, i.e., $r_{C1} \neq r_{D1}$, the interference pattern will be shifted from the symmetrical form of equation (12) according to equation (11). This interesting phenomenon has been observed and reported following the discussion of fig. 5.

To calculate the "ghost" diffraction effect of a single-slit such as shown in fig. 6, we need an integral of the effective two-photon wavefunction over the slit width:

$$R_c(x_2) \propto \left| \int_{-\frac{a}{2}}^{\frac{a}{2}} dx_0 e^{-ikr(x_0,x_2)} \right|^2 \cong sinc^2\left(\frac{x_2 \pi a}{\lambda z_2}\right) \qquad (13)$$

where $r(x_0,x_2)$ is the distance between points x_0 and x_2, x_0 belongs to the slit's plane, and the inequality $z_2 \gg a^2/\lambda$ is assumed.

Repeating the above calculations, the combined interference-diffraction coincidence counting rate for the double-slit case is given by

$$R_c(x_2) \propto sinc^2\left(\frac{x_2 \pi a}{\lambda z_2}\right) \cos^2\left(\frac{x_2 \pi d}{\lambda z_2}\right) \qquad (14)$$

which is exactly the same as equation (7) obtained from experimental data fittings. If the finite size of the detectors and the divergence of the pump are also taken into account by a convolution, the interference visibility will be reduced. These factors have been taken into account in the theoretical plots in figs. 5 and 6.

4 Acknowledgements

References

[1] E.Schrodinger, Naturwissenschaften **23**, 807, 823, 844(1935); a translation of these papers appears in *Quantum Theory and Measurement*, edited by J.A. Wheeler and W.H. Zurek, Princeton University Press, New York (1983).

[2] A. Einstein, B. Podolsky, and N. Rosen, Phys. Rev. **35**, 777 (1935).

[3] Does a single particle have defined momentum in the following state?

$$|\Psi\rangle = \sum_{i,j} \delta(\mathbf{k}_i + \mathbf{k}_j - \mathbf{k}_0)|\mathbf{k}_i\rangle|\mathbf{k}_j\rangle,$$

where $\mathbf{k}_0$ is a constant. Quantum mechanics answers: No. "no elementary quantum phenomenon is a phenomenon until it is a recorded phenomenon" [4]. EPR thought: It Should! EPR first suggested the above "perfect entangled" state, i.e., the momentum of either particle is undetermined; however, if one is measured to be $\mathbf{k}_1$ (an eigen value), then the other one is 100% determined to be $\mathbf{k}_0 - \mathbf{k}_1$, and then gave their criteria. Locality: there is no action-at-a-distance; Reality: "if, without in any way disturbing a system, we can predict with certainty the value of a physical quantity, then there exists an element of physical reality corresponding to this quantity". According to EPR's criteria, a single particle in the above state should have defined momentum. After this conclusion, EPR presented their Completeness: "every element of the physical reality must have a counterpart in the complete theory". This led to the question: "Can quantum-mechanical description of physical reality be considered complete?"

[4] W.A. Miller and J.A. Wheeler, *Foundations of Quantum Mechanics in the Light of new Technology*, edited by S. Kamefuchi *et. al.*, Physical Society of Japan, Tokyo, p.140 (1984).

[5] A. Yariv, *Quantum Electronics*, John Wiley and Sons, Inc., New York (1989).

[6] D.N. Klyshko, *Photons and Nonlinear Optics*, Gordon and Breach Science Publishers, New York (1988).

[7] See, for example, C.O. Alley and Y.H. Shih, *Foundations of Quantum Mechanics in the Light of New Technology*, edited by M. Namiki *et al.*, Physical Society of Japan, Tokyo, p.47 (1986); C.K. Hong, Z.Y. Ou, and L. Mandel, Phys. Rev. Lett. **59**, 2044 (1987); Y.H. Shih and C.O. Alley, Phys. Rev. Lett. **61**, 2921 (1988); Z.Y. Ou, and L. Mandel, Phys. Rev. Lett. **61**, 54 (1988).

[8] T.B. Pittman, Y.H. Shih, D.V. Strekalov, and A.V. Sergienko *submitted to Phys. Rev. A. Rapid Communication* (1995).

[9] D.V. Strekalov, A.V. Sergienko, D.N. Klyshko, and Y.H. Shih, Phys. Rev. Lett. **74**, 3600 (1995).

[10] For related theory, see D.N. Klyshko, Phys. Lett. **A 132**, 299 (1988); D.N. Klyshko, Sov. Phys. Usp. **31**, 74 (1988); A.V. Belinskii, and D.N. Klyshko, JETP **78**, 259 (1994).